OPEN

Correspondence and
requests for materials
should be addressed to
A.B. (antonio.bru@
mat.ucm.es)

Scaling in complex systems: a link between the dynamics of networks and growing interfaces

A. Brú[1], E. Alós[2], J. C. Nuño[3] & M. Fernández de Dios[1]

[1]Department of Applied Mathematics, Universidad Complutense de Madrid, 28040 Madrid, [2]Department of Economics and Business, Universitat Pompeu Fabra, 08005 Barcelona, Spain, [3]Department of Applied Mathematics, Universidad Politécnica de Madrid, 28040 Madrid, Spain.

We consider growing interfaces as dynamical networks whose nodes are the discrete points of the interface and the edges the physical interactions among them. We map the points of the interface formed at each time into a graph by means of a visibility algorithm. As the corresponding interfaces grow, their visibility graphs change over time. We show that the visibility graphs are all scale free for each time. We use the variance of the node degrees as a measure of the dynamical properties of these graphs. This magnitude reveals an unexpected scaling behaviour of these graphs in both the number of nodes and time. This enables to define three robust exponents that characterize any type of dynamics with more detail than the classical scaling analysis applied directly to the physical interfaces. To check the feasibility of this approach we study and classify six different dynamical processes and estimate their critical exponents. We conclude that the dynamics of physical systems far from equilibrium can be determined by its corresponding visibility network. Indeed, this methodology is able to discern among dynamical processes that hitherto have been classified in the same universality class according to the scaling analysis of their interfaces.

M any different real systems and physical phenomena have been successfully described by considering them as complex networks composed by a large number of interacting items. In this long list we can find, for instance, the World Wide Web, social networks, coupled biological and chemical systems, neural networks, social interacting species, the Internet, cell metabolism[2–4]. Although most of the real networks are dynamical, i.e. either the number of edges and nodes vary over time or there are certain attributes of the nodes and edges that change over time, the major achievements of complex networks theory have to do with their static properties, i.e. their topology[5–7,33].

In comparison with this broad research line and, in spite of the important advances attained in the first decade of the XXI century[8–11], the study of network dynamics could be considered still in its infancy. Precisely, one of the main achievements of this paper is to establish a link between the evolution of complex networks and those dynamical processes that evolve under the action of randomness and develop rough interfaces. Indeed, this outer envelope of the border can be considered as a fingerprint of the underlying dynamical processes responsible for the growth of the system. Most of the activity is carried out at the interface or "active perimeter"[1] and its geometrical properties are conserved during their evolution. Consequently, these systems possess quantities that are invariant both in time and space[12–15]. Furthermore, despite particular details that make them different, these systems can be classified into universality classes to get a global understanding of their properties. Strikingly, all well studied systems in nature belong to one of a comparatively small number of such universality classes.

In this paper, we show that the interfaces of dynamical processes can be understood as complex networks that capture the physical interactions among the different points of their contour. To construct these networks, we take into account the geometrical form of the interface and apply an algorithm of visibility to their points in order to establish their connectivity. The networks constructed from the interfaces change over time as do the interfaces. We prove that these visibility graphs exhibit scaling properties like the interfaces from which they are mapped. Importantly, the visibility algorithm is able to extract the dynamics of the processes from the invariant properties of the interfaces with greater detail than the scaling analysis of the physical processes. As a consequence, a complete characterization of the dynamical growth models is provided by the estimation of a set of critical exponents of their corresponding visibility graphs.

Dynamical growth processes

Growing surfaces and one-dimensional interfaces are formed in a wide variety of natural and artificial processes. Experimental and theoretical studies carried out in the last decade of the last century showed that most of these interfaces are rough and display a fractal nature[12,14]. Specific techniques to study critical phenomena contributed to developing this theory. In particular, the scaling hypothesis turns out to be very fruitful to obtain a qualitative description of global character. Indeed, it was proven that most of the systems belong to a short number of universality classes. Nevertheless, this analysis still left relevant questions unanswered[16].

To go further in this research, we apply the visibility network approach to studying growing interfaces that correspond to six different growth processes. Three of these models are described by continuous equations, the so called Edwards-Wilkinson (EW)[17], Kardar-Parisi-Zhang (KPZ)[18] and Molecular Beam Epitaxy (MBE)[19] and the other three are discrete models: Random Deposition (RD)[20], Random Deposition with Surface Relaxation (RDSR)[21] and the Eden model[22]. They describe a wide variety of non-equilibrium phenomena such as for example, among many others, the snow deposition on a window (RD), paper burning (EW), fluid invasion in porous media or bacterial growth (KPZ), semiconductor devices or crystal growth (MBE).

According to their dynamics and basic mechanisms, these models are characterized by the values of a set of critical exponents. Two dynamical processes with the same values of critical exponents are said to belong to the same universality class. These exponents arise from the power law behaviour of the interface local width, a measure of the local fluctuations of the height of the interface around its local average value, that is defined as follows:

$$w(l;t) = \left\{ \sqrt{ \left\langle \frac{1}{l}\sum_i h^2(i;t) - \left(\frac{1}{l}\sum_i h(i;t) \right)^2 \right\rangle_l } \right\} \quad (1)$$

where $h(i;t)$ is the height of site i at time t. Here l is the number of sites of the subsystem, in general, less than the whole length of the interface L. $<>_l$ represents the spatial average over the size l and { } denotes the average over the realizations of the noise. The width of these rough interfaces shows the scaling behavior

$$w(l,t) = \begin{cases} t^{\beta} & \text{if } t \ll t_s \\ l^{\alpha} & \text{if } t \gg t_s \end{cases} \quad (2)$$

with α the roughness exponent, β the growth exponent, and t_s a saturation time which depends on the window size. These two critical exponents are related through the scaling ansatz $z = \frac{\alpha}{\beta}$, where z is the dynamical exponent, which characterizes the time scaling behaviour of the lateral correlation length, $l_c \sim t^{1/z}$. In general, α coincides with the Hurst exponent H that describes self-affine fractals[14].

Although this description is valid for a great variety of physical processes, there exist some cases for which it is not. When the local width $w(l;t)$ differs from the global width $w(L;t)$, we can define $\alpha \equiv \alpha_{loc}$ and α_g, the local and global roughness exponents, respectively, as[23,24]:

$$w(l,t) \sim l^{\alpha_{loc}}, \; w(L,t) \sim L^{\alpha_g}, \; t \gg t_s \quad (3)$$

This global interface roughness exponent, α_g, can be obtained from the scaling of the power spectrum given by the interface Fourier transform:

$$S(q;t) = q^{-2\alpha_g - 1} s\left(q t^{\frac{1}{z}} \right) \quad (4)$$

where s is a structure factor which shows the scaling behavior:

$$s(u) = \begin{cases} const & \text{if } u \gg 1 \\ u^{2\alpha_g + 1} & \text{if } u \ll 1 \end{cases} \quad (5)$$

Any type of dynamical process evolving under the action of noise may be described by a stochastic growth equation, based on the conservation laws of the underlying dynamics, which reflects the main symmetries of the dynamics both in space and time. The simplest surface growth process is Random Deposition (RD) since no correlations exist between the points of the interface. The width of the surface grows as $w \sim t^{\frac{1}{2}}$. Therefore, $\beta = \frac{1}{2}$ (in all dimensions). In the limit of large but finite length, the continuous height-field variable $h(x; t)$ satisfies the master equation:

$$\frac{\partial h(x;t)}{\partial t} = \eta(x;t) \quad (6)$$

where $\eta(x; t)$ is a zero-average Gaussian noise with variance $\langle \eta(x; t) \eta(x'; t') \rangle = 2D\delta(x-x')\, \delta(t-t')$.

The EW represents a process where correlations spread due to diffusion only and give rise to one dimensional dynamics described by the roughness exponent $\alpha = \frac{1}{2}$ and the growth exponent $\beta = \frac{1}{4}$. As before, in the limit of large system sizes L the EW satisfies the stochastic diffusion equation:

$$\frac{\partial h(x;t)}{\partial t} = \sigma \nabla^2 h(x;t) + \eta(x;t) \quad (7)$$

Here, the parameter σ denotes the interface tension.

The KPZ describes those processes where the spread of correlations is nonlinear. The continuous KPZ stochastic equation includes a term that breaks the up-down symmetry:

$$\frac{\partial h(x;t)}{\partial t} = \sigma \nabla^2 h(x;t) + \lambda(\nabla h(x;t))^2 + \eta(x;t) \quad (8)$$

As σ, the parameter λ is non-universal. In one dimensional problems the critical exponents are known exactly[12]: $\beta = \frac{1}{3}$, $\alpha = \frac{1}{2}$ and $z = \frac{3}{2}$.

The anomalous MBE process is adequately described in the mean field approach by the master equation[25]:

$$\frac{\partial h(x;t)}{\partial t} = -k \frac{\partial^4 h(x;t)}{\partial x^4} + \eta(x;t) \quad (9)$$

where k is the interface diffusion coefficient, which is independent of the critical exponents. For the one-dimensional MBE, the critical exponents are: $\alpha_g = \frac{3}{2}$, $\beta = \frac{3}{8}$, $z = 4$ and $\alpha = 1$.

The discrete growth models have been proven a very valuable alternative to understanding the microscopic laws that are operating in the formation of the interfaces of the dynamical processes. In the simulation of Random Deposition (RD), particles are added to a randomly chosen site of the surface that, consequently, increases its height by a unit. The Random Deposition with Surface Relaxation (RDSR) includes also surface diffusion that allows particles just deposited on the interface to move to a neighbouring site with lower height. This diffusion step tends to smooth the interface and limits its maximum width w. In the so called Eden model, particles become stuck randomly to any point of the perimeter of the adjacent occupied sites (e.g. a vertex). The scaling of the growing interfaces obtained from these discrete models has been studied extensively[12,14]. It has been proven that RD, as well as its continuous counterpart, constitutes a universality dynamical class whereas RDSR and Eden models belong to the EW and KPZ universality classes, respectively.

Visibility graphs

The data set formed by the height of each point of the substrate that constitutes the interface at a given time can be transformed into a graph by applying the visibility algorithm as defined by Lacasa *et al.*[26]. Essentially, the algorithm seeks to capture the geometrical correlations that exist among the discrete points that form the one-dimensional

contour. This algorithm has been successfully applied to studying time series and it has enabled to characterize the intrinsic properties of the process that generates this data[28–31]. In particular, the visibility graph associated to fractal time series has provided an alternative way of computing their Hurst exponent[27]. Specifically, given a discrete interface at time t, where the height of each point of a one-dimensional substrate is given by $h(k; t)$, the natural visibility graph at time t is created as follows: (i) a node in the graph is associated to each point k, (ii) two nodes are connected if visibility exists, i. e. if a visibility line is not intersected by any intermediate data height. Formally, two different nodes i and j of the graph are connected at time t if for the corresponding points in the interface $(i; h(i; t))$ and $(j, h(j; t))$ no other points $i < k < j$ with heights $h(k; t)$ verify:

$$h(k; t) < h(j; t) + (h(i; t) - h(j; t))\frac{j-k}{j-i} \qquad (10)$$

Figure 1 depicts schematically how the algorithm works to obtain the natural visibility graph from the interface at various times. By definition, these visibility graphs have the same number of nodes as the number of points in the discrete substrate, i.e. their size is $N = L$, for all times. Moreover, since each node sees at least its nearest neighbors and the links have no direction, the visibility graphs are connected and undirected. It is worth to noting that the graph is invariant under affine transformation of the interface data. For each realization, the interfaces of the continuous processes EW, KPZ and MBE are obtained from the numerical integration using the classical finite difference method[32] of the corresponding master equation. The size of the substrate is always taken as $L = 4096$ and the final time for each simulation is $T = 10^4$. The simulations of the discrete growth models RD, RDSR and Eden are performed following the standard procedures[12]. In these cases, we carry out the simulations with 10^7 particles

and take an arbitrary time scale that corresponds to the deposition of 10^3 particles. Thus, the total number of time steps is $T = 10^4$.

A first measure to characterize the visibility graph is given by the connectivity of the network. The total number of connections of node i with other nodes, denoted by k_i, is its connectivity degree. The probability distribution of connectivity degrees of a network is referred to as the degree distribution, $P(k)$. It gives the probability that a randomly selected node has exactly k nodes. Figure 2 shows the degree distributions of the natural visibility graphs that correspond to the interfaces for the six dynamical processes at different times. As it can be seen, all the distributions converge for long times. Importantly, all curves depict a power law dependence that proves the scale-free character of the visibility graphs[39]. Besides, the exponents of the power law differ among the dynamical processes: $\gamma_{EW} \approx$ 2.1 for the Edwards-Wilkinson and $\gamma_{KPZ} \approx 2.07$ for the Kardar-Parisi-Zhang. The degree distributions for the discrete models are: $\gamma_{RD} \approx 3.14$ for the Random Deposition, $\gamma_{RDSR} \approx 2.46$ for the Random Deposition with Surface Relaxation and $\gamma_{Eden} \approx 2.25$ for the Eden model. The degree distribution for the anomalous MBE exhibits two regimes with different exponents: for low values of k $\gamma_{MBE1} \approx 0.9$, whereas for larger values of the connectivity degree k, $\gamma_{MBE2} \approx 3.0$.

As it was proven in[27], the exponents of these power laws provide a rigorous estimation of the Hurst (α) exponent of the fractal interfaces through the relation: $2\alpha = 3 - \gamma$. The validity of this expression is restricted to those processes that yield a value of $\alpha \in [0, 1]$. This is the case for EW and KPZ: $\alpha_{EW} \approx 0.45$ and $\alpha_{KPZ} \approx 0.47$ and for RDSR and Eden: $\alpha_{RDSR} \approx 0.27$ and $\alpha_{Eden} \approx 0.38$. These estimations are close to their theoretical values for EW and KPZ ($\alpha = 0.5$ for both processes). On the contrary, the estimations do not coincide for the discrete models RDSR and Eden that, theoretically, ought to have the same α-value. For the other two classes their power law exponents yield a null value for both α_{RD} and α_{MBE} for RD and for the second regime (large k values) that appear for MBE, respectively. Nonetheless, for lower values of k (first k-regime), the exponent of the MBE degree distribution is $\gamma \approx 1$ which gives a Hurst exponent $\alpha = 1$ that equals the theoretical value of α for this process.

Network scaling

In order to obtain a deeper characterization of these dynamical processes we require a dynamical magnitude associated to the network evolution. We find it in the classical network theory where it is already defined as the analogue to the interface local width: the variance of the vertex degree[35]. If we take a node subset $n \leq N$ we define the local variance of the vertex degree as:

$$W(n; t) = \left\{ \sqrt{\left\langle \frac{1}{n}\sum_i k_i^2(t) - \left(\frac{1}{n}\sum_i k_i(t)\right)^2 \right\rangle_n} \right\} \qquad (11)$$

where the averages are defined as in Equation (1) but over a subset of nodes. Note that, by construction, the total number of nodes N coincides with the interface total length L. A similar definition can be applied for the global variance of the degree vertex if we replace n by N. The global variance of a random graph was originally related to the "irregularity" or heterogeneity of the network[34,36] and, in agreement with the geometrical interpretation of the visibility graph, it is going to reproduce the scaling behaviour of the interface width w. Indeed, as Figures 3 and 4 show, the variance of the vertex degrees follows the scaling law:

$$W(n; t) \approx t^b \qquad (12)$$

for early times, and

$$W(n; t) \approx n^a \qquad (13)$$

for long enough times. Here, a and b represent the local variance and dynamical variance of the visibility graph, which are analogous to the
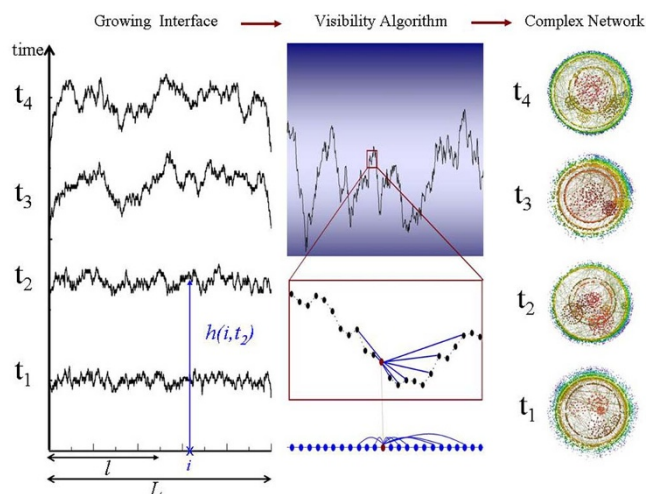

Figure 1 | Illustration of the visibility algorithm that converts for each time step a growing interface into a complex network. *Left*: A growing interface on a substrate of size L at four times. It can be described by a continuous function, $h(x, t)$ which represents the height of point or angle x at time t. *Middle*: An interface is represented at any time of its evolution by a corresponding complex network by applying the visibility algorithm and which is formed with the same number of nodes N as the interface length L. A point of the interface is considered as a node in the visibility graph which is connected to those nodes that are visible from its heights h. *Right*: Based on the connectivity of each node, k_i, we present an schematic visualization of the networks corresponding to the interfaces of the MBE dynamics at four different times under the k-core representation, which enables to disentangle the hierarchical structure of the networks by progressively focusing on their central cores.
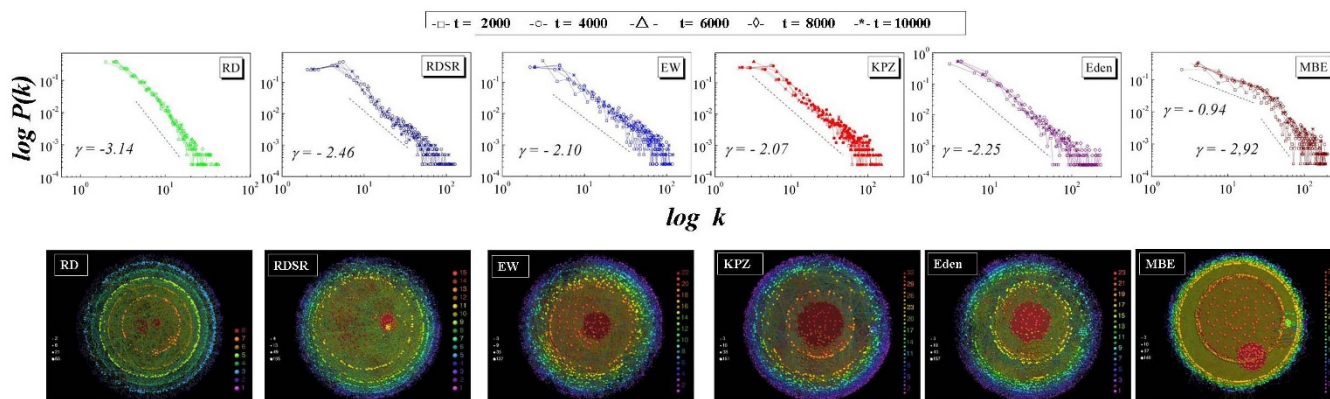
Figure 2 | Degree distributions of the natural visibility graphs built from the interfaces at time $t = 5000$ for the six types of dynamical processes, as obtained by numerical integration of the corresponding continuous master equation for: (EW) Edwards-Wilkinson, (KPZ) Kardar-Parisi-Zhang and (MBE) Molecular Beam Epitaxy and from the simulation of the discrete models: Random Deposition (RD), Random Deposition with Surface Relaxation (RDSR) and Eden model. As it can be seen, the six degree distributions exhibit a power law dependence but with different exponents. An estimation of the Hurst (α) exponents of each process can be obtained from the exponent of their power law distributions by means of the relation[27]: $2\alpha = 3 - \gamma$. Concretely, $\alpha_{EW} \approx 0.45$, $\alpha_{RDSR} \approx 0.27$ $\alpha_{KPZ} \approx 0.47$ and $\alpha_{Eden} \approx 0.38$. The estimation for RD is $\alpha_{RD} \approx 0$. Note that the degree distribution of the visibility graph corresponding to MBE presents two regimes for low and large values of k. The first part of the distribution provides $\alpha_{MBE} \approx 1.032$, a value that is compatible with the theoretical prediction. The second part of the distribution yields $\alpha^*_{MBE} \approx 0.04$, similar to RD. Below each figure the corresponding k-core decomposition of the visibility graph is depicted (see main text).

roughness and growth exponents of the interface width. These exponents can be estimated from the representation of W as a function of the network size and time, respectively. Figure 3 depicts how W depends on the network size for $0 < n \leq N$ for the six dynamical processes. As it can be observed, W shows a similar dependence as the interface width w: it increases linearly for low values of n and it saturates when n approaches the total network size N. This behaviour is characteristic of the scaling properties of W and it allows to calculate the scaling exponent a from the slope of the straight line that fits the data for initial times. In order to estimate the growth exponent b for each of the dynamical processes, we determine the visibility graphs for the interfaces formed at 100 time-steps equally elapsed from 0 to 10^4 and we perform over 10 system realizations to reduce the noise effects. As it can be appreciated in Fig. 4, for initial times the variance W behaves linearly with a slope whose value depends on the type of dynamical growth process from which the visibility graph is built. This slope corresponds to the scaling exponent b in equation (12). As expected, the lowest value of b corresponds to the Random Deposition, i.e. $b_{RD} \approx 0$, whereas the largest value corresponds to MBE, $b_{MBE} \approx 0.25$. The processes EW and KPZ have an exponent $b_{EW} \approx 0.11$ and $b_{KPZ} \approx 0.17$, respectively. The critical exponents for the other discrete models are: $b_{RDSR} \approx 0.15$ and $b_{Eden} \approx 0.23$. Theses results are summarized in Table 1. Note that the critical exponents obtained for RDSR and Eden models differ significantly from those that correspond to EW and KPZ, which are the universality classes that classical analysis assigns respectively to these discrete models[12,14]. This result stresses the relevance of this network approach to discover unknown properties of the kind of dynamical processes that have not been discovered using classical methods.

A third critical exponent can be obtained from the power spectrum of the connectivity of the nodes of the visibility graph to determine its global scaling properties. Fig. 5 shows the log-log representation of the discrete power spectrum S for the corresponding visibility graphs of each of the models at a given time. As it can be seen, the power spectrum behaves according to a scaling law for the six dynamical processes. Concretely, if the discrete power spectrum scales as:

$$S(q; t) \sim q^{-c} \qquad (14)$$

then, the global exponents of each of the process are given by: $c_{RD} = \approx 0.07$ for Random Deposition, both EW and KPZ have similar values: $c_{EW} \approx 0.70$ and $c_{KPZ} \approx 0.76$. The MBE growth process has $c_{MBE} \approx 2.15$. The corresponding exponents of two discrete models are: $c_{RDSR} \approx 0.63$ and $c_{Eden} \approx 0.87$.

The representation of the visibility graph constructed from the growing interfaces yields other perspective about the universality classes. In particular, the k-core decomposition splits the network into components with distinct connectivity and, quite likely, with specific functionality[40,41]. This technique consists of identifying particular subsets of the network, called k-cores, each one obtained by a recursive pruning strategy. A k-core of a network can therefore be obtained by recursively removing all the vertices of degree less than k, until all vertices in the remaining graph have degree at least k. Consequently, more central cores are more strongly connected, with large number of distinct paths between vertices. Figure 2 shows the k-cores decomposition for each of the models addressed in this paper for at time $t = 5000$. Note that all vertices in a shell are drawn with the same colour. A graduate colour scale is used to represent and to distinguish different k-cores, from the k_{min} to the k_{max}. Each shell has a certain radial width that depends on the correlations properties of the vertices in the shell.

At first glance, notable differences are appreciated among them showing the distinct mechanisms of formation behind each of the visibility graphs. A closer inspection reveals the differences in the density of connections that is larger in the MBE-visibility graph and lower in the corresponding to Random Deposition. It is also worth mentioning the propensity to form clusters in inner k-cores in EW and KPZ visibility graphs. Besides, it is in these two networks where the width of the k-cores is larger. These two properties show up an internal structure that is less notorious in RD and MBE visibility graphs. We can observe a correlation between the core index and the connectivity degree meaning that more central nodes are likely high-degree hubs of the visibility graph. Lastly, it is interesting to note the presence of a nucleus, with all nodes in the k_{max}-shell, in all the graphs except the RD-visibility graph. Nonetheless, this nucleus is not exactly located at the center of the decomposition as occurs for EW, KPZ and Eden visibility graphs. All the decompositions have an external structure formed mainly by isolated nodes that are connected to the rest of the network basically through the immediately larger k-shells.
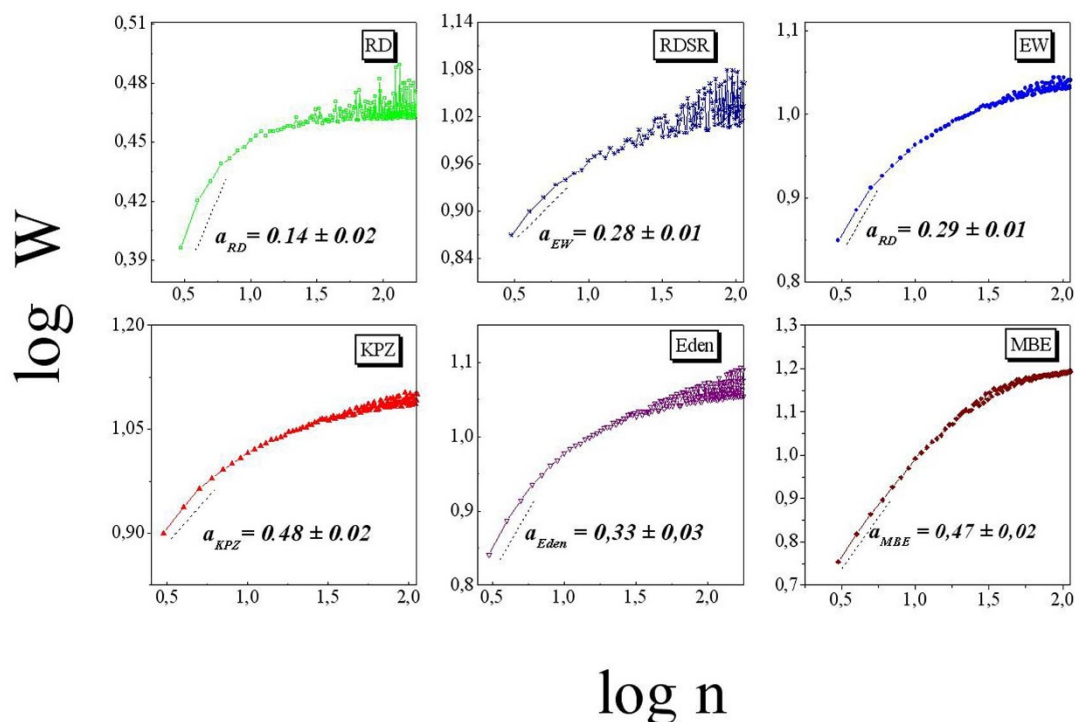
Figure 3 | Log-Log representation of the variance of the node degrees *W* as a function of the network size *n* of the visibility graph corresponding to interfaces at time *t* = 5000. At this time, the interfaces of all the processes, except RD, are already saturated and, therefore, the slope at the origin determines the scaling exponent *a*. According with the classical scaling theory of growing interfaces KPZ and Eden belong to the same universality class defined by the roughness exponent $\alpha = 0.5$. On the contrary, the value of the exponent *a* for Eden and KPZ differs appreciably, $a_{KPZ} \approx 0.48$ and $a_{Eden} \approx 0.33$. The exponent for RD is $a_{RD} \approx 0.14$ which contrasts with the corresponding roughness exponent equal to 0. The value of the MBE exponent is $a_{MBE} \approx 0.47$. The results are obtained after averaging over 10 realizations.
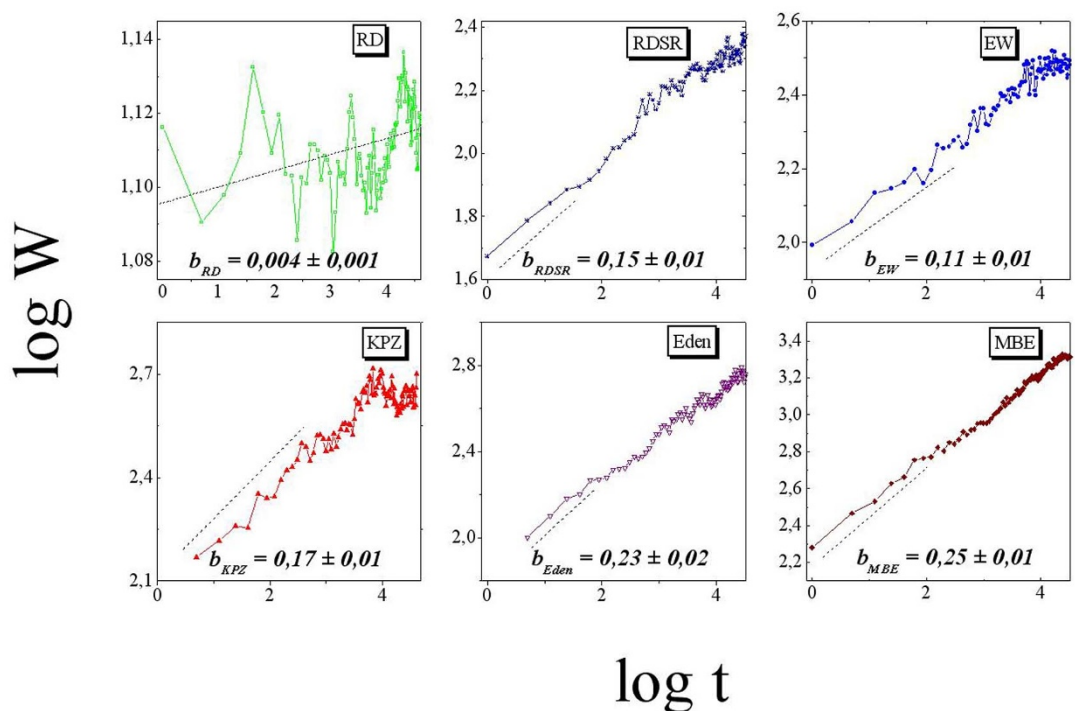

Figure 4 | Log-log representation of the variance of the vertex degrees *W* as a function of time for the visibility graphs obtained from interfaces for the six growth processes studied. The initial slope of the curves determines the scaling exponent *b*. One hundred visibility graphs, each one obtained from the corresponding interface at this time step, are analyzed. As it can be seen, a clear power law dependence appear for the six models. As it occurs with the critical exponent *a*, this exponent allows to discriminate between process that, according with the classical theory should have the same exponent.

Table 1 | Critical exponents obtained from the scaling of the width of the growing interfaces (Classical exponents) and from the scaling of the variance of the node degrees of the corresponding visibility graph (Network exponents) for each of the dynamical processes studied in this paper

dynamical Process	Network exponents	Classical exponents
RD	$a = 0.14$, $b = 0.004$, $c = 0.07$	α not defined $\beta = \frac{1}{2}$
EW	$a = 0.12$, $b = 0.28$, $c = 0.79$	$\alpha = \frac{1}{2}$ $\beta = \frac{1}{4}$
KPZ	$a = 0.29$, $b = 0.14$, $c = 0.76$	$\alpha = \frac{1}{2}$ $\beta = \frac{1}{3}$
MBE	$a = 0.48$, $b = 0.25$, $c = 2.12$	$\alpha_g = \frac{3}{2}$, $\alpha = 1$ $\beta = \frac{3}{8}$ $\beta^* = \beta - \frac{\alpha_{loc}}{z} = \frac{1}{8}$
RDSR	$a = 0.28$, $b = 0.15$, $c = 0.63$	$\alpha = \frac{1}{2}$ $\beta = \frac{1}{4}$
Eden	$a = 0.33$, $b = 0.23$, $c = 0.87$	$\alpha = \frac{1}{2}$ $\beta = \frac{1}{3}$

Concluding remarks

In this paper we have shown that the interfaces of growing dynamical processes can be described as complex networks whose nodes are points of the interface and the links correspond to physical interactions (visibility) among them. The number of connections among the nodes change over time as a consequence of the evolution of the contours. A mapping from the data set provided by the interface into a graph can be done at each time step using the natural visibility algorithm[26]. The application of this network methodology enables to uncover hidden properties, both geometrical and temporal, of the interface that remain invariant as the interface grows. In analogy with the classical scaling theory, this invariance has been detected in the analysis of the variance of the vertex degrees of the visibility graphs. This variance was already used as a measure of the irregularity of complex networks[34–36]. In reference to this magnitude, the dynamics of the visibility graph can be classified as a function of the two critical exponents: a and b. The third exponent c is directly computed from the power spectrum of the connectivity of the nodes of the corresponding visibility graph.

To check whether this methodology is able to distinguish among different dynamics that, in principle, can belong to the same universality class, we have studied six different growth models, both discrete (Random Deposition, Random Deposition with Surface Diffusion and Eden model) and continuous (Edwards-Wilkinson,
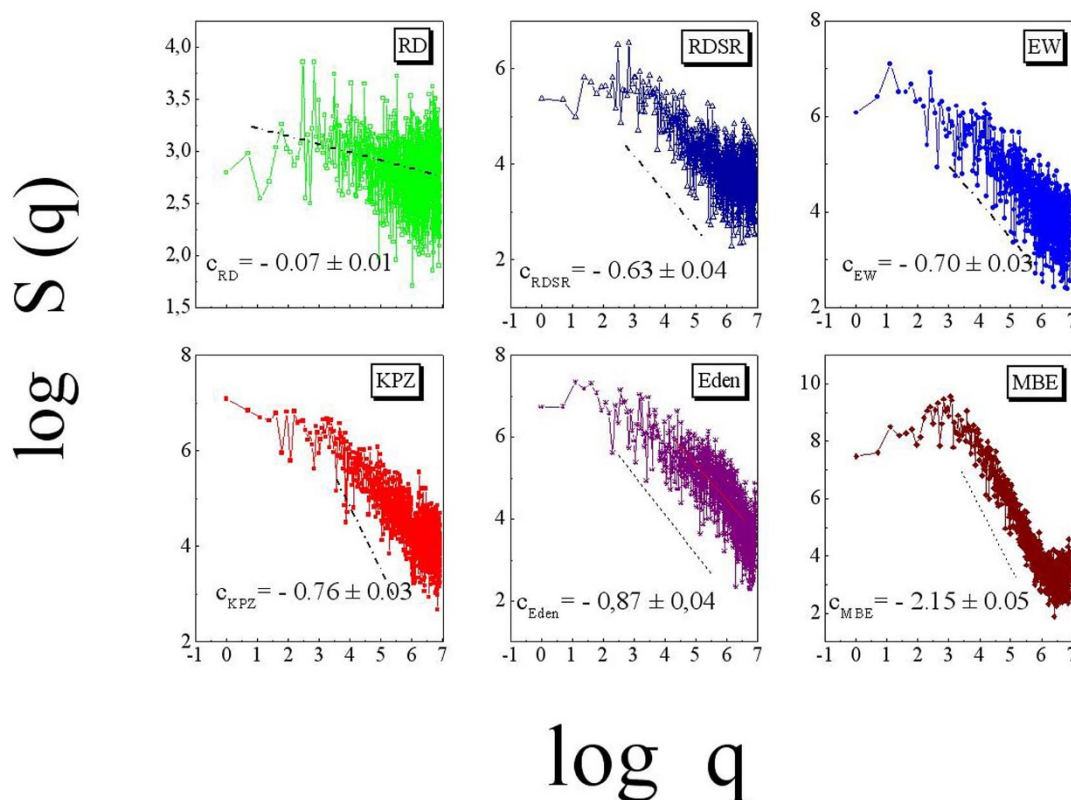

Figure 5 | **Log-log representation of the power spectrum of the variance of the node degrees of the six processes studied in this paper.** We can estimate the "global variance" of the vertex degrees from the global behaviour of the power spectrum of the visibility graphs, obtained in a similar way as in (4), distinguishes clearly among the six dynamical processes. While RD has got $c_{RD} \approx 0.07$, both EW and KPZ have a scaling exponents $c_{EW} \approx 0.70$ and $c_{KPZ} \approx 0.76$. The process MBE has $c_{MBE} \approx 2.15$. The other two discrete models yield: $c_{RDSR} \approx 0.63$ and $c_{Eden} \approx 0.87$. The interfaces used for the calculations were taken at time $t = 10^4$.

Kardar-Parisi-Zhang and Molecular Beam Epitaxy). Indeed, this approach is able to discriminate between dynamics that are considered in the same universality class, e.g. Eden and KPZ and RDSR and EW, as can be seen in Table 1. The discrepancies that have been detected from the scaling analysis of the visibility graph reveal that the classical classification of dynamical growth processes needs to be reconsidered[37,38]. To conclude, we would like to stress the feasibility of this methodology for studying the dynamical properties of real systems: with a set of experimental data we can carry out a straightforward construction of the corresponding visibility graphs and then, to get its dynamical properties and classification in a universality class. Further investigations are required to find out whether there exists a new relationship among the critical exponents that describe the dynamical characteristics of the visibility graphs. We trust that the application of this network approach to other non-equilibrium systems can discover these compelling theoretical questions.

1. Leyvraz, F. The "active perimeter" in cluster growth models: a rigorous bound. *J. Phys. A: Math. Gen.* **18**, L941–L945 (1985).
2. Barabasi, A. L. *Linked:The New Science of Networks* (Perseus Press, Cambridge, 2002).
3. Watts, D. J. *Six Degrees: the Science of a Connected Age.* (Random House, London, 2003).
4. Csermely, P. *Weak Links. The Universal Key to the Stability of Networks and Complex Systems* (Springer-Verlag, Berlin, 2009).
5. Caldarelli, G. *Scale Free Networks. Complex Webs in Nature and Technology* (Oxford University Press, Oxford, 2007).
6. Cohen, R. & Havlin, S. *Complex Networks Structure, Robustness and Function* (Cambridge University Press, Cambridge, 2010).
7. Estrada, E. *The Structure of Complex Networks. Theory and Applications* (Oxford University Press, New York, 2011).
8. Durrett, R. *Random Graph dynamics* (Cambridge University Press, Cambridge, 2007).
9. Pastor-Satorras, R. & Vespignani, A. *Evolution and Structure of the Internet. A Statistical Approach* (Cambridge University Press, New York, 2004).
10. Mukherjee, A., Choudhury, M., Peruani, F., Ganguly, N. & Mitra, B. (Eds.) *dynamics On and Of Complex Networks, Volume 2 Applications to Time-Varying dynamical Systems* (Springer Science Business Media, New York, 2013).
11. Lu, X. B. & Qin, B. Z. *Syncronization in Complex Networks.* (Nova Science Publishers, New York, 2011).
12. Barabási, A. L. & Stanley, H. E. *Fractal Concepts in Surface Growth* (Cambridge University Press, Cambridge, 1995).
13. Ódor, G. Universality classes in nonequilibrium lattice systems. *Rev. Mod. Phys.*, **76** (2004).
14. Meakin, P. *Fractals, Scaling and Growth far from Equilibrium* (Cambridge University Press, Cambridge, 1998).
15. Krug, J. Origins of scale invariance in growth processes. *Adv. Phys.* **46**, 139–282 (1997).
16. Kolakowska, A. Deciphering dynamical patterns of growth processes. *Eur. J. Phys.* **30**, 1353–1364 (2009).
17. Edwards, S. F. & Wilkinson, D. R. The Surface Statistics of a Granular Aggregate. *Proc. R. Soc. London A* **381**, 17–31 (1982).
18. Kardar, M., Parisi, G. & Zhang, Y.-C. Dynamic scaling of growing Interfaces. *Phys. Rev. Lett.*, **56**, 889–892 (1986).
19. Das Sarma, S. & Tamborenea, P. A new universality for kinetic growth: one-dimensional Molecular Beam Epitaxy. *Phys. Rev. Lett.*, **66**, 325–328 (1991).
20. Family, F. & Viscek, T. Scaling of the active zone in the Eden process on percolation networks and the ballistic deposition model. *J. Phys. A: Math. Gen.* **18**, L75 (1985).
21. Family, F. Scaling of rough surfaces: effects of surface diffusion. *J. Phys. A: Math. Gen.* **19**, L441–L446 (1986).
22. Eden, M. *A two-dimensional growth process*, in Proceedings of the fourth Berkeley Symposium on Mathematical Statistics and Probability Volume IV: Biology and problems of health [Neyman, J. (ed.)] [223–239] (University of California Press, Berkeley, 1961).
23. Brú, A., Pastor, J. M., Fernaud, I., Melle, S. & Brú, I. Super-rough dynamics on tumour growth. *Phys. Rev. Lett.* **81**, 4008–4011 (1998).
24. López, J. M., Rodríguez, M. A. & Cuerno, R. Super-roughening versus intrinsic anomalous scaling of surfaces. *Phys. Rev. E* **56**, 3993–3998 (1997).
25. Lai, Z. W. & Das Sarma, S. Kinetic roughening with surface relaxation: Continuum versus atomistic models. *Phys, Rev. Lett* **66**, 2348–2351 (1991).
26. Lacasa, L., Luque, B., Ballesteros, F., Luque, J. & Nuño, J. C. From time series to complex networks: The visibility graph. *PNAS* **105** (2008).
27. Lacasa, L., Luque, B., Luque, J. & Nuño, J. C. The Visibility Graph: a new method for estimating the Hurst exponent of fractional Brownian motion. *Europhys. Lett.* **86**, 30001 (2009).
28. Lacasa, L. & Toral, R. Description of stochastic and chaotic series using visibility graphs. *Phys. Rev. E* **82**, 036120 (2010).
29. Luque, B., Lacasa, L., Ballesteros, F. J. & Robledo, A. Feigenbaum graphs: a complex network perspective of chaos. *PLoS ONE* **6** (2011).
30. Lacasa, L., Nuñez, A., Roldán, E., Parrondo, J. M. R. & Luque, B. Time series irreversibility: a visibility graph approach. *Eur. Phys. J. B* **85** (2012).
31. Nuñez, A. M., Lacasa, L., Gomez, J. P. & Luque, B. Visibility algorithms: A short review, in: *New Frontiers in Graph Theory*, edited by: Zhang, Y., InTech, Rijeka, Chapter **6**, 119152, doi:10.5772/34810 (2012).
32. Virieux, J. P-SV wave propagation in heterogeneous media: Velocity-stress finite-difference method. *Geophysics* **51**, 889–901 (1986).
33. Newman, M. E. J. The structure and function of networks. *SIAM Rev.* **45**, 167–256 (2003).
34. Bell, F. K. A Note on the Irregularity of Graphs. *Linear Algebra Appl.* **161**, 45–54 (1992).
35. Estrada, E. Quantifying network heterogeneity. *Phys.Rev. E* **82**, 066102 (2010).
36. Snijders, T. A. B. The degree variance: An index of graph heterogeneity. *Soc. Networks* **3**, 163–174 (1981).
37. Nicoli, M., Cuerno, R. & Castro, M. Dimensional fragility of the Kardar-Parisi-Zhang universality class. *J. Stat. Mech.* doi:10.1088/1742-5468/2013/11/P11001 (2013).
38. Katzav, E. & Schwartz, M. What is the connection between ballistic deposition and the Kardar-Parisi-Zhang equation? *Phys. Rev. E* **70**, 061608 (2004).
39. Barabási, A. L. & Albert, R. Emergence of scaling in random networks. *Science* **286**, 509–512 (1999).
40. Alvarez-Hamelin, I., Dall'Asta, L., Barrat, A. & Vespignani, A. LaNet-vi in a Nutshell. http://lanet-vi.soic.indiana.edu/lanetvi-22.pdf (2006) Date of access:26/09/2014.
41. Dorogovtsev, S. N., Goltsev, A. V. & Mendes, J. F. F. k-core percolation and k-core organization of complex networks. *Phys. Rev. Lett.* **96**, 1–4 (2006).

Author contributions

A.B. and J.C.N. wrote the main manuscript text and prepared the figures and tables. All authors analyzed the data and reviewed the manuscript. A.B., E.A. and M.F.D. performed the simulations.

Additional information